Int J Adv Manuf Technol (2017) 91:1339–1345
DOI 10.1007/s00170-016-9838-z

ORIGINAL ARTICLE

Synthesis and characterization of 3C-SiC by rapid silica carbothermal reduction

M. Barbouche[1,4] · R. Benabderrahmane Zaghouani[2] · N. E. Benammar[3] · K. Khirouni[4] · H. Ezzaouia[4]

Received: 12 July 2016 / Accepted: 25 November 2016 / Published online: 6 December 2016

Abstract In this work, rapid carbothermal reduction of silica in a homemade electric arc furnace is reported to produce silicon carbide intended for photovoltaic applications. The influence of carbothermal conditions on the composition and size of the obtained particles is studied. We demonstrate that the variation of the temperature and the atmosphere makes it possible to produce 3C-SiC powders during a short time. Morphological properties of the elaborated SiC powder were investigated using laser granulometry and scanning electron microscopy (SEM). The obtained samples are composed of agglomerated particles of different shapes with micrometric sizes. X-ray diffraction (XRD), fourier transform infrared (FTIR), and Raman spectroscopy analyses show that carbothermal reduction of silica depends on the experimental conditions. Especially, the sample elaborated during 120 s at 1700 °C under CO atmosphere does not present any SiO_2 peaks but only pure crystallized cubic silicon carbide (β-SiC) with crystallite size around 44 nm as a result of a complete carbo-reduction of silica. The purity of synthesized SiC is investigated by inductively coupled plasma atomic emission spectrometry (ICP-AES) giving rise to purity about 97.9927%.

Keywords Silicon carbide · Carbothermal reduction · Structural characterization · Morphological characterization · Purity analysis

✉ M. Barbouche
barbouchemed@gmail.com

[1] Laboratory of Nanomaterials and Systems for Renewable Energy, Research and Technologies Centre of Energy, Technopark of Borj-Cedria, BP 95, 2050 Hammam-Lif, Tunisia

[2] Photovoltaic Laboratory, Research and Technologies Centre of Energy, Technopark of Borj-Cedria, BP 95, 2050 Hammam-Lif, Tunisia

[3] Laboratory of Valuation of Useful Materials, National Center of Research in Material Science, Tunis, Tunisia

[4] Laboratory of Semiconductor, Nanostructure and New Technologies, Research and Technologies Centre of Energy, Technopark of Borj-Cedria, BP 95, 2050 Hammam-Lif, Tunisia

1 Introduction

Silicon carbide (SiC) has recently generated much interest. As a wide band gap semiconductor, it possesses interesting optical, physical, and electrical properties that make it as a perfect candidate for several industrial and engineering applications. In particular, nanostructured SiC including nanospheres, nanowires, and nonorods has paved the way for new functional materials for nanoscale engineering. Among a number of possible structures of SiC, the cubic 3C (β-SiC) and the hexagonal 6H and 4H (α-SiC) are mostly studied until now. They present a wide band gap spectrum covering the visible–ultraviolet range: 2.39, 3.02, and 3.26 eV for 3C, 6H, and 4H, respectively [1]. Specially, the β-SiC exhibits mechanical strength, high ionic mobility, thermal stability, chemical inertness, and high saturation electron drift velocity encouraging its integration in ceramic and abrasive industry and high-temperature and high-frequency semiconducting devices [2–5]. Many techniques are proposed in order to synthesize SiC nanoparticles such as the ball milling of silicon and

carbon-mixed powders [6] and the carbothermal reduction of silica [7, 8]. Several research works have reported on the use of the carbothermal reduction of silica as it is known to be a simple and economical process for silicon carbide nanostructures elaboration [8]. Wang et al. have produced SiC nanoparticles with size ranging from 20 to 60 nm in a sealed tube furnace equipped with a vacuum pump at a temperature of 1450 °C during 5 h under argon atmosphere [9]. Guo et al. have also obtained SiC powders with characteristic shapes for ceramic applications by carbothermal reduction of silica and bamboo charcoal under argon atmosphere [10]. With a temperature increase, the authors have observed the SiC crystal shape transformation from string-beads-like to dumbbell-like and rod-like. Furthermore, Shin et al. have reported on the use of mineralized wood with silica in acidic conditions followed by carbothermal reduction in argon atmosphere to obtain crystalline SiC nanoparticles (200–700 nm) [11]. Crystalline 2H-SiC nanoribbons of over a hundred microns in length and 30–100 nm in thickness were also obtained by Zhang et al. using silicon powder and carbon black powder in a horizontal alumina tube heated by a tubular furnace at 1500 °C under argon atmosphere [12]. β-SiC nanoparticles ranging from 10 to 40 nm obtained by carbothermal reduction of silica with graphite in a microwave furnace at 1450 °C during 60 min have been reported by Moshtaghioun et al. [13]. In this work, we report on the production of SiC powder by rapid carbothermal reduction of silica intended to be used as a target to deposit a SiC passivation layer on silicon for photovoltaic applications. The elaboration of SiC powder is carried out in a homemade electric arc furnace. The effect of the processing parameters such as the temperature and the atmosphere on the formation of SiC powder is investigated.

2 Experimental

2.1 Sample preparation

Silicon carbide powder was produced by carbothermal reduction using silica with purity of 99.898% [14] and carbon powder taken from coal with a nominal molar ratio $C/SiO_2 = 3/1$. The overall reaction for the SiC formation through carbothermal reduction of silica is depicted by Eq. ((1)):

$$SiO_2(s) + 3C(s) \leftrightarrows SiC(s) + 2CO\ (g) \quad (1)$$

Prior to the production of SiC, silica and carbon powders were mixed for more homogeneity. The silica reduction is performed in a homemade electric arc furnace (Fig. 1) under different atmospheres (air; inert gas, argon; and reducing gas, CO) and different temperatures during a short time (120 s).

The experimental conditions are resumed in Table 1.

Fig. 1 A photograph of the homemade electric arc furnace

The powder mixture loaded in a graphite crucible is placed without tamping into the hot zone of the furnace, and the gas is introduced into the reaction chamber during the experiment. The temperature regulation is performed using a temperature controller "OMRON E5AK." The experimental procedure is recapitulated in Fig. 2.

2.2 Characterization

The obtained material properties depend on a variety of factors including the furnace temperature, the atmosphere, and the process duration. In order to optimize SiC synthesis, the effect of each of these parameters on its electrical and optical properties is analyzed. The crystalline structure as well as the crystallite size and the lattice parameters was determined by an XRD "PANalytical X'pert Pro MPD" diffractometer equipped with a copper Kα (λ = 0.154 nm) radiation source. To identify the presence of SiC bands, a FTIR "Nicolet MAGNA-IR 560" spectrometer in a transmittance mode was used. The obtained powder were ground, dispersed in a matrix of KBr at room temperature, and pressed into pellets. More information about the polytype structure of SiC is investigated by a Raman "LabRAM HR JOBIN YVON Technology HORIBA Scientific" spectrometer. Synthesized SiC particle size and morphology are analyzed by laser granulometry and SEM. Purity of synthesized SiC and

Table 1 Different conditions of SiC production

Sample	B	C	D	E
Temperature (°C)	1500	1700	1700	1700
Atmosphere	Air	Air	Argon	CO
Duration (s)	120	120	120	120

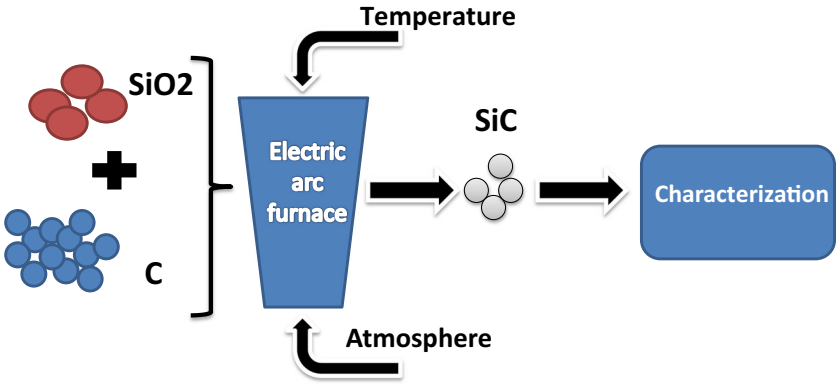

Fig. 2 Schematic representation of SiC production

commercial SiC were analyzed by inductively coupled plasma atomic emission spectrometry (ICP–AES).

3 Results and discussion

3.1 Morphology analysis

Figure 3 shows SiC particle size distribution measured by a laser granulometry technique.

The synthesized SiC particles have a wide size distribution ranging from 7 μm to 1 mm. The majority of the particles have the size in the range of 50–500 μm. Average particle size is about 100 μm. SEM images of samples synthesized at different conditions are illustrated in Fig. 4. As shown, all samples are composed of agglomerated particles with different sizes and shapes. The obtained particles have micrometric sizes confirming the laser granulometry results.

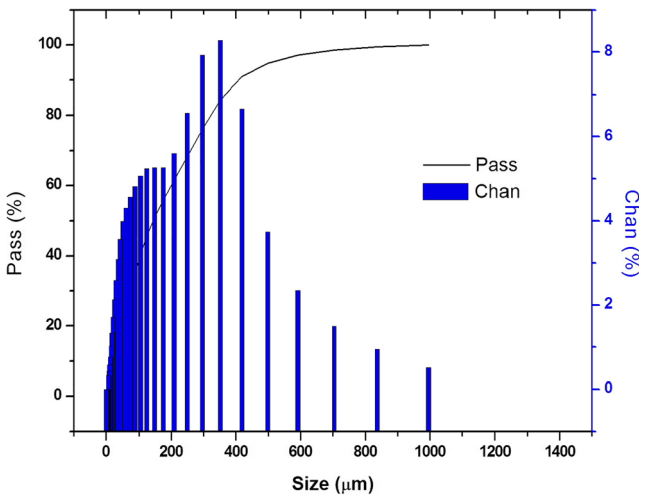

Fig. 3 SiC particle size distribution

3.2 X-ray diffraction analysis, grain crystallinity, and size

The key point to obtain crystalline SiC particles is the deep understanding of the elaboration mechanism and then the good optimization of experimental parameters. In Fig. 5, we compare the X-ray diffraction patterns of the reactant SiO_2 and the samples obtained under different conditions as resumed in Table 1.

We notice that the sample B synthesized at 1500 °C under air presents only SiO_2 peaks and no peak of SiC is detected. However, when the temperature is increased to 1700 °C (sample C), we note the apparition of small peaks attributed to SiC around $2\theta = 35.4°$, $2\theta = 60°$, and $2\theta = 71.1°$. But the major peaks are still associated to SiO_2 explained by an incomplete reduction of silica to SiC. An increase of the temperature or a change of the atmosphere is essential. We choose to keep the temperature at 1700 °C and to work under argon atmosphere (sample D). We remark the appearance of SiC principal peaks around $2\theta = 35.4°$, $2\theta = 60°$, and $2\theta = 41.2°$ corresponding respectively to (111), (200), and (220) phases of 3C-SiC as reported in the literature [4, 10, 11, 15]. We notice the persistence of SiO_2 peaks attributed also to the incomplete process due to its short duration. The use of a reducing gas such as CO may accelerate silica reduction. Samples elaborated under condition E do not present any SiO_2 peaks but only sharp SiC peaks indicating the crystallinity of obtained silicon carbide. We distinguish peaks corresponding to (111), (200), (220), and (311) phases of 3C-SiC with a maximum intensity of the (111) peak.

Using the Bragg equations (Eqs. (2) and (3)), the lattice parameter of 4.396 Å and the interplanar spacing d_{111} of 2.539 Å are obtained from the (111) diffraction plane: values close to those reported for the 3C-SiC in the literature [11, 16].

$$d = \frac{a}{\sqrt{\left(h^2 + k^2 + l^2\right)}} \tag{2}$$

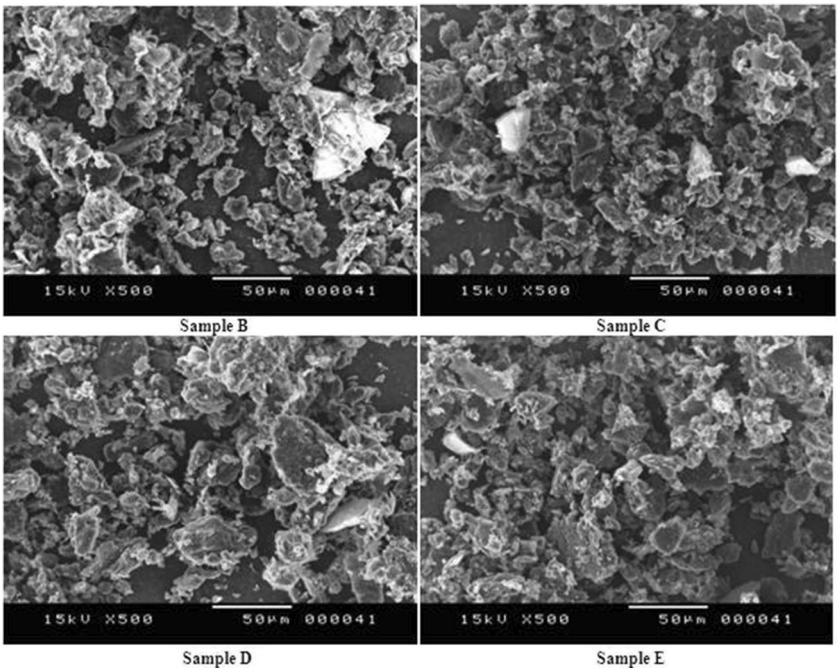

Fig. 4 SEM images of synthesized samples under different conditions

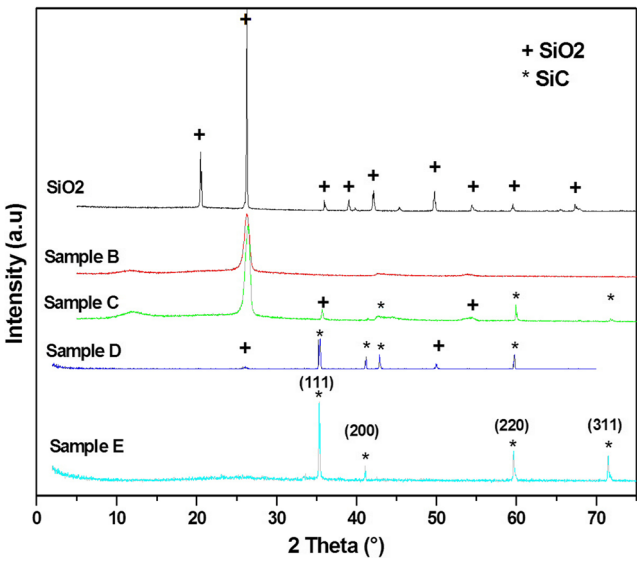

Fig. 5 XRD patterns of used SiO_2 and produced SiC at different conditions

$$d = \frac{n\lambda}{2sin\theta} \tag{3}$$

We have also determined the average crystallite size using the Scherrer formula assuming a spherical shape of the crystallites (Eq. (4)) [17–19].

$$s = \frac{K\lambda}{\beta cos2\theta} \tag{4}$$

where K is a constant (K = 0.9), λ is the X-ray wavelength (λ = 1.5406 Å) and β is the line broadening at half the maximum intensity (FWHM). Table 2 recapitulates the average crystallite size of the different samples.

The SiO_2 crystallite size decreases with the increase of temperature and the change of the atmosphere due to the reduction of silica. By changing the atmosphere from air to the reducing gas (CO), the size of produced SiC particles decreases from 90 to 44 nm, thanks to a better reduction of SiO_2 and formation of SiC. Under condition E, the β-SiC is obtained.

3.3 FTIR analysis

Figure 6 shows infrared spectra of samples synthesized under the different processing conditions in a transmittance mode.

Table 2 Evolution of crystallite size with synthesis conditions

Sample	SiO_2	B	C	D	E
SiO_2 average crystallite size (nm)	63.349	14.24	12.58	11.173	0
SiC average crystallite size (nm)	–	0	90.949	43.807	44.399
Crystallite produced	–	SiO_2	SiO_2 + β-SiC	SiO_2 + β-SiC	β-SiC

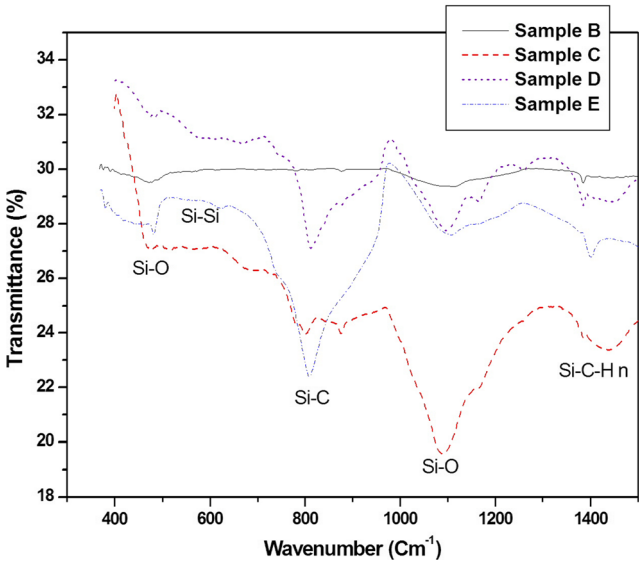

Fig. 6 FTIR spectra of samples synthesized under different conditions

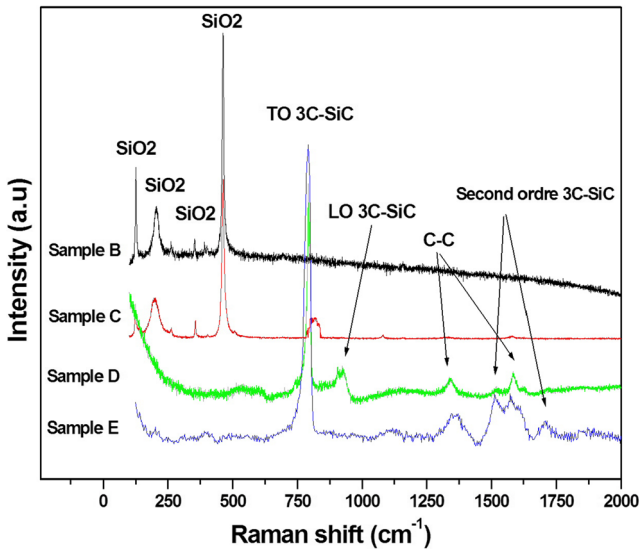

Fig. 7 Raman spectra of different samples

We notice the presence of three vibration modes for the sample B: two principal bands at 480 and 1100 cm^{-1} are attributed to SiO binding [20] and a small band located about 1385 cm^{-1} corresponding to the Si–CHn vibration mode [21]. When performing at condition C, we notice the reduction of peaks associated to the Si–O band around 480 cm^{-1}proving a partial reduction of silica. We notice also the presence of a peak around 800 cm^{-1} attributed to Si–C band [4, 22]. The partial reduction of silica is also noticed for the sample synthesized under condition D which shows the presence of a Si–C principal peak at 800 cm^{-1} and the persistence of a Si–O peak with considerable intensity. The sample synthesized at temperature of 1700 °C under CO during 120 s presents a Si–C dominant peak around 800 cm^{-1} referred to the transversal optic (TO) mode of the 3C-SiC crystalline phase [23]. The FTIR analysis confirms the results obtained by XRD.

3.4 Raman analysis

The SiC particles were further studied by Raman spectroscopy. Raman scattering is a powerful and non-destructive tool, which can be used in identifying the polytype structure of SiC [24]. In Fig. 7, we show the Raman spectra of the different samples.

We notice for sample B, the presence of peaks at 125, 207, 351, and 463 cm^{-1} attributed to SiO_2 [25, 26]. The same peaks are observed for sample C with an additional peak at 810 cm^{-1} corresponding to 3C-SiC. For samples D and E, the dominant peak is located at 795 cm^{-1} attributed to a SiC TO mode confirming that elaborated SiC particles consist mainly of cubic polytype structure [24, 27, 28]. Moreover for sample E, we notice additional peaks around 1500 and 1712 cm^{-1} considered second-order or combinational bands of β-SiC [27, 28]. Peaks situated at 1360 and 1578 cm^{-1} can be attributed to the phonon modes of C–C bonding [28, 29]. Raman results are in agreement with the results obtained by XRD and FTIR.

3.5 Purity analysis

To reach high-efficiency silicon-based solar cells, many materials have been reported to passivate silicon. Recently, silicon carbide has been proposed as a passivation layer for silicon by the field-effect passivation and/or the saturation of the

Table 3 ICP–AES analysis of the synthesized SiCElement

	Ni	Pb	S	Sr	Zn	Mo	Nb	P	Ti	Li
Concentration (ppm)	1.814	<0.001	16.490	<0.001	5.644	3.023	2.015	33.058	4.434	6.652
Element	Co	Cd	Ca	Be	Ba	B	Al	Ta	Na	Tl
Concentration (ppm)	2.418	1.411	630.122	5.644	1.411	12.094	41.121	8.466	2515.65	27.615
Element	Ge	Fe	Cu	Cr	K	Mg	Mn	Re	Ga	Total
Concentration (ppm)	2.822	20.762	9.272	1.209	89.902	115.3	0.806	5.241	34.267	20072.18
Purity (%)	97.9927									

dangling bonds at the silicon interface [30]. For this purpose, the elaborated SiC powder is intended to be used as a target for SiC deposition on silicon. A purity analysis by ICP–AES spectrometry to quantify the major SiC impurities present in the powder is necessary. Table 3 resumes the concentrations of different impurities present in synthesized SiC powder.

As we can conclude, the quality of our elaborated SiC is comparable to synthesized SiC powders obtained in the literature [31, 32].

4 Conclusion

Rapid carbothermal reduction of silica in a homemade electric arc furnace to produce silicon carbide is discussed. Different experimental conditions have been applied. In particular, the temperature and the atmosphere are shown to be key parameters in the reduction of silica. Under different conditions, the obtained powder is consisting of micrometric particles. It was found that processing at 1700 °C under CO atmosphere is the most favorable to obtain a complete conversion of SiO_2 to silicon carbide during a short time (120 s). The XRD, FTIR, and Raman investigations of the produced material show the disappearance of SiO_2-related peaks and the presence of Si–C ones. Crystallized cubic silicon carbide (β-SiC) with crystallite size about 44 nm was obtained at 1700 °C under CO atmosphere indicating a successful and complete conversion of SiO_2 into SiC during a short processing time. The obtained SiC powder has a purity of 97.9927%, a result comparable to that obtained in the literature encouraging its use as a target for SiC passivation layer deposition on silicon for solar cell applications.

References

1. L Carassiti (2011) Synthesis of silicon carbide ceramics by novel microwave methods, PhD thesis
2. Sarro PM (2000) Silicon carbide as a new MEMS technology. Sensors & Actuators A 82:210–218
3. Jiang L, Cheung R, Hedley J, Hassan M, Harris AJ, Burdess JS, Mehregany M, Zorman CA (2006) SiC cantilever resonators with electrothermal actuation. Sensors & Actuators A 128:376–386
4. Meenakshi CH (2011) Synthesis of nano-structured 3C-SiC by carbothermal reduction of silicon bearing gel and carbon soot. Materials letter 65:2161–2164
5. Pang Q, Xu L, Ju Z, Xing Z, Yang L, Hao Q, Qian Y (2010) 3C-SiC nanowires and micro-scaled polyhedra: synthesis, characterization and properties. J Alloys Compd 501:60–66
6. Yang XY, Huang ZW, Wu YK, Ye HQ (2001) HREM observations of the synthesized proces of nano-sized SiC by ball milling of Si and C mixed powders. Materials Science Engineering A 300:278–283
7. M Barbouche, M Hajji, F Krout, H Ezzaouia (2015) Elaboration and characterization of metallurgical silicon for photovoltaic applications. J Phys Conf Ser. 596
8. M Barbouche, M Hajji, R Chtourou, H Ezzaouia (2015) Electric arc furnace design and construction for metallurgical and semiconductor research. Int J Adv Manuf Technol
9. Wang K, Cheng YB, Wang H (2009) Growth of SiC whiskers by carbothermal reduction of mesoporous silica-carbon composites infiltrated with SiC nuclei. J Aust Ceram Soc 45(1):10–12
10. Guo X, Zhu L, Li W, Yang H (2013) Preparation of SiC powders by carbothermal reduction with bamboo charcoal as renewable carbon source. Journal of Advanced Ceramics 2(2):128–134
11. Shin Y, Wang C, Exarhos GJ (2005) Synthesis of SiC ceramics by the carbothermal reduction of mineralized wood with silica. Adv Mater 17:73–77
12. Zhang H, Ding W, Li M (2010) Synthesis and characterization of crystalline silicon carbide nanoribbons. Nanoscale Res Lett 5(8): 1264–1271
13. Moshtaghioun BM, Poyato R, Rodriguez AD (2012) Rapid carbothermic synthesis of silicon carbide nano powders by using microwave heating. Journal of European ceramic society 32(8): 1787–1794
14. M Khalifa, M Hajji, H Ezzaouia (2012) Impurity removal process for high-purity silica production by acid leaching. EDP Sciences
15. Rajarao R, Ferreira R (2014) Synthesis of silicon carbide nanoparticles by using electronic waste as a carbon source. Mater Lett 120: 65–68
16. Moshtaghioun BM, Monshi A, Abbasi MH, Karimzadeh F (2011) A study on the effects of silica particle size and milling time on synthesis of silicon carbide nanoparticles by carbothermic reduction. J Refract Met Hard Mater 29:645–650
17. Monshi A, Foroughi MR, Monshi MR (2012) Modified Scherrer equation to estimate more accurately nano-crystallite size using XRD. World Journal of Nano Science and Engineering 2:154–160
18. Dehghanzadeh M, Ataie A, Heshmati-Manesh S (2012) Synthesis of nanosize silicon carbide powder by carbothermal reduction of SiO2. International Journal of Modern Physics: Conference Series 5:263–269
19. Uwe H, Neil G (2011) The Scherrer equation versus the 'Debye-Scherrer equation'. Nat Nanotechnol 6(9):534
20. Prabhakaran PV (2009) Silicon carbide wires of nano to sub-micron size from phenol-furfuraldehyde resin. Jouranl Mater Sci 44:528–533
21. Janz S (2006) Amorphous silicon carbide for photovoltaic applications. In: Masters physics. Fraunhofer Institut, Freiburg, p. 22
22. Manocha LM, Yasuda E, Tanabe Y, Manocha S, Vashistha D (2000) Sol–gel processing of carbidic glasses. Bull Mater Sci 23:1–4
23. Liao LS, Bao XM, Yang ZF, Min NB (1995) Intense blue emission from porous β-SiC formed on C + implanted silicon. Appl Phys Lett 66:2382–2384
24. Wasyluk J, Perova TS (2010) Raman investigation of different polytypes in SiC thin films grown by solid-gas phase epitaxy on Si (111) and 6H-SiC substrates. Materials Science Forum Vols 645-648:359–362
25. Alessi A, Agnello S, Buscarino G, Gelardi FM (2013) Structural properties of core and surface of silica nanoparticles investigated by Raman spectroscopy. J Raman Spectrosc 44:810–816
26. Kingma KJ, Hemley RJ (1994) Raman spectroscopic study of microcrystalline silica. Am Mineral 79:269–273
27. Qiang X, Li H, Zhang Y, Tian S, Wei J (2013) Synthesis and Raman scattering of SiC nanowires decorated with SiC polycrystalline nanoparticles. Materials Letter 107:315–317
28. Jeong J, Chung GS (2008) Raman scattering investigation of polycrystalline 3C-SiC film deposited on SiO2 by using APCVD with hexamethyldisilane. Journal of the Korean Physical Society 52:45

29. JY Zhou, ZY Chen, M Zhou, XP Gao, EQ Xie (2009) SiC nanorods grown on electrospun nanofibers using Tb as catalyst: fabrication, characterization, and photoluminescence properties. Nanoscale Res Lett
30. Martin I, Vetter M, Garin M, Orpella A, Voz C, Puigdollers J, Alcubilla R (2005) Crystalline silicon surface passivation with amorphous SiCx: H films deposited by plasma-enhanced chemical-vapor deposition. J Appl Phys 98:114912
31. Wang L, Peng Y, Hu X, Xu X (2013) Combustion synthesis of high purity SiC powder by radio-frequency heating. Ceram Int 39:6867–6875
32. Augustine G, Balakrishna V, Brandt CD (2001) Growth and characterization of high-purity SiC single crystals. J Cryst Growth 211: 339–342